Geophysical Research Letters

RESEARCH LETTER
10.1029/2023GL104761

Does Downscaling Improve the Performance of Urban Ozone Modeling?

Yuting Wang[1], Guy P. Brasseur[1,2,3], Yong-Feng Ma[4], Vincent-Henri Peuch[5], and Tao Wang[1]

[1]Department of Civil and Environmental Engineering, The Hong Kong Polytechnic University, Hung Hom, Hong Kong, [2]Max Planck Institute for Meteorology, Hamburg, Germany, [3]Atmospheric Chemistry Observation & Modeling Laboratory, National Center for Atmospheric Research, Boulder, CO, USA, [4]Department of Mechanics & Aerospace Engineering, Southern University of Science and Technology, Shenzhen, China, [5]European Centre for Medium-Range Weather Forecasts, Reading, UK

Key Points:

- Increasing horizontal resolution to 33 m improves the prediction of NO_X near the traffic emissions
- The threshold of the model resolution is around 300 m for areas with a distance to the pollution sources
- The changes of model performances with varied resolutions are different for NO_X and O_3

Supporting Information:

Supporting Information may be found in the online version of this article.

Correspondence to:

Y. Wang and G. P. Brasseur,
yuting.wang@polyu.edu.hk;
guy.brasseur@mpimet.mpg.de

Citation:

Wang, Y., Brasseur, G. P., Ma, Y.-F., Peuch, V.-H., & Wang, T. (2023). Does downscaling improve the performance of urban ozone modeling? *Geophysical Research Letters*, *50*, e2023GL104761. https://doi.org/10.1029/2023GL104761

Received 2 JUN 2023
Accepted 18 NOV 2023

Author Contributions:

Conceptualization: Yuting Wang, Guy P. Brasseur
Funding acquisition: Tao Wang
Methodology: Yuting Wang
Software: Yuting Wang, Yong-Feng Ma
Supervision: Guy P. Brasseur
Validation: Yuting Wang, Yong-Feng Ma
Visualization: Yong-Feng Ma
Writing – original draft: Yuting Wang, Guy P. Brasseur
Writing – review & editing: Yuting Wang, Guy P. Brasseur, Yong-Feng Ma, Vincent-Henri Peuch, Tao Wang

Abstract

Increasing the model resolution is expected to be one way for improving air quality forecasts in urban areas. In this study, we evaluate the model performance in a large city at various resolutions to examine the best resolution for air pollution simulations. The comparison with measurements at a station near the traffic emissions shows the advantage of using high resolutions for capturing the extreme values. The statistical evaluation indicates that the highest model resolution (33 m) provides the best results for NO_X concentration distributions near the traffic roads, while the improvement for roadside O_3 with decreasing grid spacing stops at a certain point. The best model performance for the areas with a distance to the pollution sources is with the resolution of 100–300 m, at which the transport errors are equivalent to the emission biases.

Plain Language Summary

As the increasing needs in the air quality forecasting in large cities, there is a trend in decreasing the model grid spacing to obtain more detailed pollutants distributions between neighborhoods or at street levels. To determine at which resolution the model can obtain the best representation of the pollutants' concentrations, we evaluate the model performance at different resolutions taking Hong Kong as an illustration. The analysis shows that the improvement with increasing model resolution is not monotonic for the areas far away from the intense emissions; however, the model with the highest resolution (33 m) reproduces the best results for the short-lived species near the pollution sources.

1. Introduction

Forecasting air quality in a spatially inhomogeneous metropolitan area is not straightforward. The spatial and temporal distribution of chemically interacting species inside the urban canopy depends on an array of forcing factors and is affected by internal processes: surface emissions, wet and dry deposition, multi-scale transport including advective, convective and other smaller scale turbulent motions, as well as in situ chemical and physical transformations. The accuracy of an air quality forecast in a metropolitan area is therefore directly affected by the horizontal grid size adopted in the model, the spatial and temporal resolution of the emission inventory, and the adoption of an urban canopy model. The air quality forecast is also strongly affected by the accuracy of the predicted meteorological (dynamics and physics) fields, which are influenced by the complex urban surface features, especially the building geometry in large cities. Even though the nonlinear chemical scheme characterizing tropospheric chemistry, and specifically the production rate of tropospheric ozone, is deterministic, the chaotic nature of multi-scale turbulent motions introduces random high-frequency variations in the calculated chemical fields (Y. Wang et al., 2021, 2022). A possible approach is to formulate turbulent effects either through direct numerical simulation (DNS) or large eddy simulation (LES) approaches.

Different modeling approaches have been adopted to produce deterministic air quality forecasts at the urban scale. For example, the Copernicus Atmosphere Monitoring Service system integrated in the operational Integrated Forecasting System of the European Centre for Middle-Range Weather Forecast provides global chemical fields predicted for the next few days ahead (Flemming et al., 2015). The advantage of such system is that it represents the long-distant influences on local air composition, while accounting for local chemical processes. The disadvantage is that the spatial resolution of such models is limited by the available computer resources and does not allow to resolve the specific processes characterizing urban areas. In this type of models, the effects of turbulence

on large-scale motions are either ignored or parameterized by applying a Reynolds averaging procedure to the continuity, momentum, and energy equations.

Different methods are available to downscale coarse-resolution model results and to provide a more detailed view of the chemical and dynamical systems in the regions of interests (i.e., urban areas). One approach is to make use of a high-resolution regional chemical model with lateral boundary conditions provided by the coarser global model. A typical horizontal resolution for such models is of the order of 2–15 km. Another approach is to use a global model with an unstructured grid designed with a zooming capability in the geographical region of interest (Pfister et al., 2020). With these two approaches, dynamical and chemical features can be resolved within a few kilometers, if the spatial resolution of the chemical emissions is of comparable size. However, the comparison between concentrations calculated by these types of models and measured at surface stations often exhibit deficiencies resulting from too coarse grid resolution, so that statistical corrections or further downscaling need to be applied (Guillas et al., 2008).

Further downscaling at the sub-urban size (city block or at the street level) requires that mechanically or thermally driven turbulent motions, which often become dominant, be explicitly represented. A possible approach is to perform a DNS, but the computational cost of such method is often prohibitive; therefore, LES in which the large eddy motions are explicitly resolved while the smaller eddies below a specified cut-off limit are parameterized, are often preferred. Many previous studies applied LES formulation in computational fluid dynamics (CFD) models to investigate the micro-scale processes with resolved buildings (e.g., Kwak et al., 2015; Zheng et al., 2015). However, the CFD domains are usually limited to a few kilometers squared. Recently, several meteorological LES models have been developed with coupled atmospheric chemistry such as the Parallelized Large-eddy Simulation Model (PALM, Khan et al., 2021). Specialized street models are also being considered (e.g., Kim et al., 2018; Lugon et al., 2020; T. Wang et al., 2022), but they do not include a formulation of the physical processes of turbulence.

It is generally assumed that the performance of an atmospheric model increases with the spatial and temporal resolution adopted in this model. However, some previous studies have suggested that higher model resolution does not necessarily improve the prediction accuracy. For instance, based on their simulations of ozone in two Italian cities, Falasca and Curci (2018) noted that increasing the horizontal resolution of their model to about 4 km provides a clear advantage, but that a further computational effort to run the model at a 1 km resolution is not justified. They attributed this to the error accumulation in the meteorological fields, since the same emission input was adopted in their simulations. Valari and Menut (2008) showed that the ozone concentrations calculated by their mesoscale model do not improve monotonically with the adopted spatial resolution. The fact that the results become less accurate beyond a certain resolution is attributed to the errors associated with parameterization of subgrid processes, which overcomes the benefit of the high model resolution. In the present study, rather than basing our analysis on a subgrid parameterization, we imbed in the regional model a more physically based LES formulation and assess the benefit of this approach.

Actually, the evaluation scores for the model resolution depend largely on the scales of the dominant atmospheric motions. Mass et al. (2002) discussed the roles of decreasing grid spacing under various situations, and pointed out that high resolution (at global/regional scale) is most useful for strongly forced convection (e.g., associated with topography). When further going down to the scale of less than 1 km in space or 1 hr in time, the complex nonlinear turbulent motions become crucial, and the introduction of LES brings in the advantages of representing the small-scale structures. For instance, Muñoz-Esparza et al. (2017) compared their coupled meso-to-microscale simulations to wind lidar profiles and surface measurements, demonstrating that LES provides a better representation of the PBL structure. Thomas and Kurzeja (2023) evaluated the model capability of tracer transport at mesoscale, grayscale, and LES scale, and indicated that LES exhibits the best agreement with observations. In addition to the accuracy of the meteorological fields, which is essential for the transport of atmospheric chemical species, the complexity of the emission distributions also plays a significant role. Valari and Menut (2008) found that the resolution of the emission fluxes is the dominant factor that affects air quality simulations. Joe et al. (2014) evaluated the impact of increasing model resolution with LES on the particle dispersion in a densely populated area, and indicated that the high resolution does not improve the prediction everywhere in the study domain, but can resolve extreme values near the sources. However, an evaluation of the model resolution with the inclusion of an embedded LES has not been applied to atmospheric chemistry, since the number of studies with realistic LES coupled chemistry is still limited.

In this paper, we examine the relation between the performance of a coupled mesoscale-microscale modeling system that includes a chemical module applied to a metropolitan area and the adopted horizontal resolution of the model. In this study, we focus on the high model resolution aspects provided by the LES module, so that the present study can be viewed as an extension of the previous air quality model evaluations focusing on global to regional scales. The study is conducted in the urbanized region of Hong Kong, which has been chosen because it is characterized by large heterogeneities in land cover, topography, and surface emissions, strong turbulent and convective motions, and active photochemistry. In addition, beyond a given spatial threshold, the dominant high-frequency random motions make it very difficult to perform a one-to-one comparison of calculated species concentrations with measurements made at selected air quality stations, and statistical methods must be introduced to validate the model results. The availability of a large number of air quality measurement stations operated by the Hong Kong government provides the data needed to perform a statistical evaluation of the model results.

2. Materials and Methods

We simulate the dynamical and chemical fields using version 4.0.2 of the Weather Research and Forecasting (WRF) Model (Skamarock et al., 2019) coupled with chemistry (Grell et al., 2005). Details about the modeling system and its evaluation are provided by Y. Wang et al. (2023). The main model configurations are listed in Table S1 in Supporting Information S1.

Different spatial grid resolutions covering the domain of Hong Kong (Figure S1 in Supporting Information S1) are being considered: 2.7 km (noted D03), 900 m (D04), 300 m (D05), 100 m (D06), and ultimately 33 m (D07). When considering the high-resolution cases D05–D07 (inner domain), an LES module is inserted in the modeling system. The formulation of vertical exchanges in the PBL of the mesoscale model is based on the Yonsei University scheme (Hong et al., 2006). In the LES module, the large eddies are fully resolved, while the effects of the small eddies are parameterized using the 1.5 order closure of Deardorff (1970). To accurately represent the PBL turbulent processes, we have selected a particular day (1 August 2018) characterized by a typical convective boundary layer.

The adopted photochemical and chemical mechanism is based on the second-generation Regional Acid Deposition Model (RADM2, Stockwell et al., 1990). In the mesoscale model, several emission inventories are adopted to cover the whole domain. The details can be found in Text S1 in Supporting Information S1. In the inner domains, more detailed vehicle emissions for every road, point emissions of power plants, industries, crematoriums, and tank farms are used and interpolated to the model resolutions. As an illustration, the gridded emission maps of NO for different domains are shown in Figure S2 in Supporting Information S1.

Several chemical species including nitrogen oxides (NO_X) and ozone (O_3) are continuously measured at 16 monitoring stations located in the Hong Kong territory. For this particular study, we examine the simulated concentrations using observations, only taking the road monitoring site of Central located in a busy area on the north side of Hong Kong Island as an example. Detailed comparison and analysis of other sites was shown in the paper by Y. Wang et al. (2023).

The meteorological measurements at the surface stations operated by the Hong Kong Observatory are used to evaluate the model performance from the point of view of meteorology. The map of the stations considered here is shown in Figure S3 in Supporting Information S1. Since the chemical and meteorological observations are not co-located, we focus on the statistical evaluation for the meteorology and link it with the chemical simulations.

3. Results

In Figure 1, we first show two components (horizontal and vertical) of the wind velocities as well as the concentrations of ozone and NO_X calculated as a function of time, and compare these model values with the corresponding quantities measured at Central Station during the simulation periods. The wind velocities are displayed in the two lowest panels for two specific spatial resolutions of the model: 900 m (mesoscale model) and 33 m (LES model), respectively. The time evolution of the NO_X and ozone concentrations at the same two spatial resolutions are displayed in the upper two panels. These upper panels also show the hourly averaged concentrations of the two chemical species at the same location as calculated for all five model cases with different spatial resolutions. As

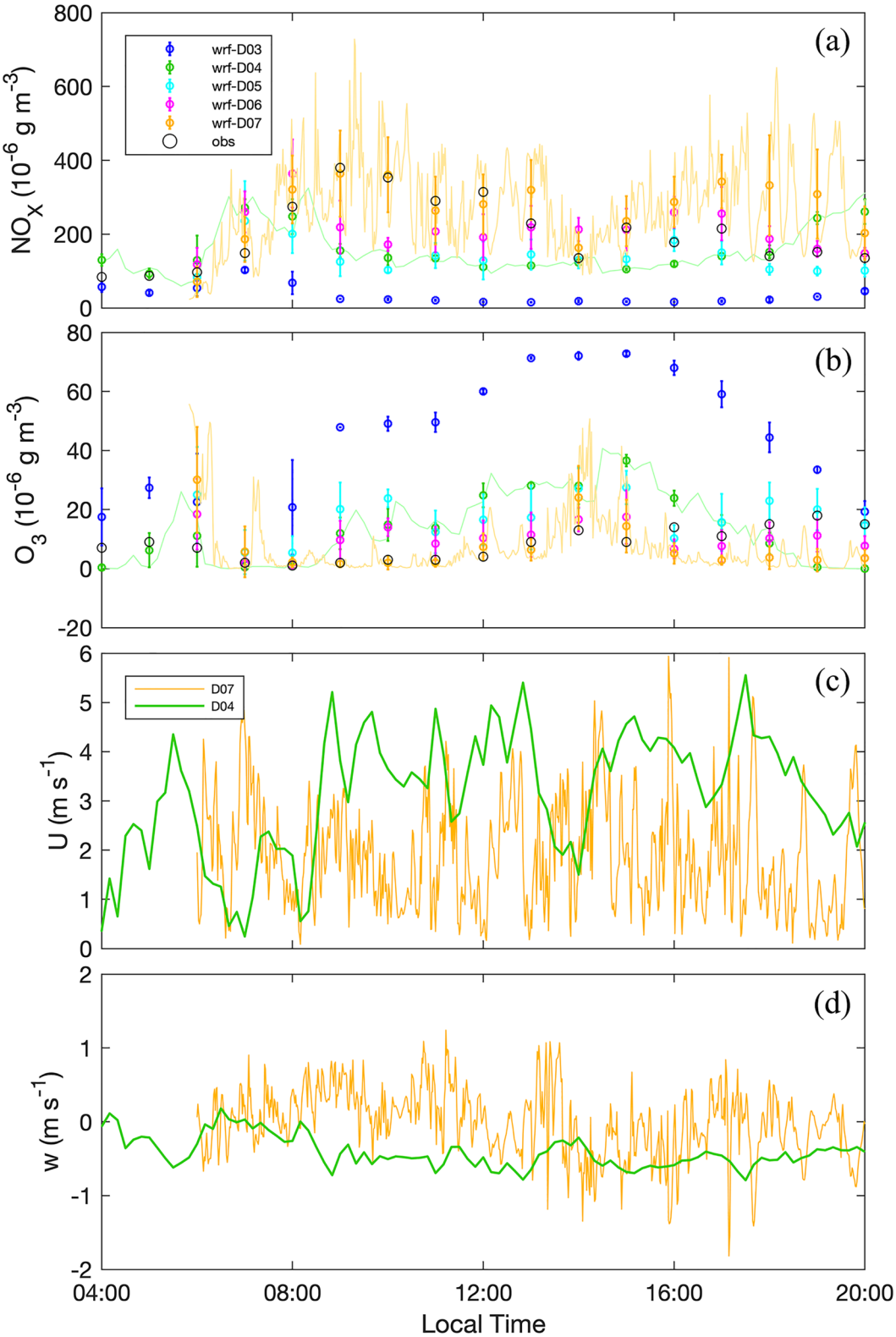

Figure 1. Comparison between simulations and measurements for (a) NO_X and (b) O_3 at Central Station. Dots with error bars are hourly means of simulations (blue: D03, 2,700 m; green: D04, 900 m; cyan: D05, 300 m; magenta: D06, 100 m; and yellow: D07, 33.3 m) with the standard deviations. Black circles are hourly measurements. Solid lines are the model output at corresponding temporal intervals (10 min for D04 and 1 min for D07). (c) Horizontal and (d) vertical wind speed at the first model layer from D04 and D07 output.

expected and by design, the results obtained at 33 m resolution based on the LES approach exhibit considerably more variability (turbulence) than the quantities derived by the mesoscale model at 900 m resolution. Further, the hourly averaged concentrations of NO_X and ozone are not identical when considering the predicted low- and high-resolution values, respectively. Specifically, in the case of NO_X, the high-resolution values generated by the LES model at Central Station are higher than those reproduced by the mesoscale model, and the value of the hourly mean concentration increases with the model resolution. The best agreement with observations is provided by the model with the highest resolution. This suggests that, for short-lived species at a busy location in the middle of the city, the high-resolution model better represents the evolution of the hourly mean concentrations derived from measurements. This is consistent with the findings in Joe et al. (2014). In the case of O_3, the situation is opposite to that of NO_X: the calculated hourly averaged concentrations are reduced when the model resolution increases. This is explained by the fact that, in the very polluted area of Central, ozone is titrated by NO. Here again, the agreement between simulated and measured concentrations is best when the model resolution is highest.

Finally, we examine some statistical parameters that provide a measure of the quality of the simulations performed at different resolutions taking into account data from the different monitoring stations in Hong Kong. We focus on the Mean Bias (MB), the Root Mean Square Error (RMSE), and the Correlation Coefficient (r). In our analysis, we distinguish between stations established along busy roads (called roadside stations) and other stations (called general stations). Figure 2 represents the relationships between the simulated and observed concentration values for all stations (displayed in black dashed lines), for roadside stations (displayed in red solid lines), and for general stations covered by D06 (displayed in cyan solid lines). We also add the linear fit lines obtained at the three general stations included in the smallest domain D07 (displayed in blue solid lines). The parameters for the least squares regressions are listed in Table S2 in Supporting Information S1.

When considering all stations, the slope of the linear least squares regression line for NO_X from stations included in the adopted domain varies as a function of the spatial resolution, with values of 0.19, 0.61, 0.58, 0.81, and 0.85. The model results therefore improve as the spatial resolution increases. If one refers only to the road stations, which are very much affected by the localized traffic emissions, the NO_X slope changes to 0.13, 0.49, 0.45, 0.65, and 0.82. The relationship between model and measured NO_X data at road stations is worse than that when considering all stations, since the models do not capture the high concentration values. When the resolution reaches 33 m, the performance of the model improves with regard to NO_X, although the data are more scattered with larger unsystematic RMSE (RMSEu). This can be explained by the large variability in the turbulent flows resolved in the high-resolution LES.

In the case of the longer-lived ozone, the values of the slope for increasing resolutions do not vary substantially with the model resolution; they are 1.55, 1.08, 1.05, 0.96, and 0.92. When considering road stations only, the corresponding values of the slope are 4.71, 1.89, 1.68, 1.10, and 1.06. In this case, the improvement of the model performance with increasing resolution is clearer; however, the model with the 33 m resolution shows a similar result to that with the 100 m resolution. It indicates that in the polluted area the simulated O_3 is less sensitive to the model resolution than NO_X after the resolution increases to a certain point.

To exclude the large bias at the roadside stations, we also examine the model behavior for the general stations only. For consistency in the sample numbers among the model resolutions, we first consider the three general stations included in all the domains. The derived slopes of the linear regression lines for NO_X are 0.42, 1.66, 1.67, 1.88, and 2.20. Different from the roadside stations, the model performance improves at first but becomes worse again as the grid size decreases. The best result appears at the 300 m model resolution, since it provides a much better correlation coefficient than the 900 m model. In the case of O_3, the obtained slopes from the three general sites are 1.39, 0.93, 0.96, 0.81, and 0.91. The model with 300 m resolution also provides the best result, implying that at this resolution the errors from the emissions and the transport have a comparable magnitude. To gain better credibility with more data, the regression fit from the general stations covered by the D06 is also provided. The best results are found at the 300 m resolution for NO_X, and at 100–300 m for O_3.

The values of MB, RSME, and the correlation coefficient for the different cases are provided in Table 1. In the case of the roadside stations, the MB for NO_X and ozone decreases as the model resolution increases. The same behavior is found for the RMSE with one exception: in the case of ozone, the value of the RMSE increases when the resolution increases from 100 to 33 m. Moreover, the correlation coefficient for O_3 decreases from 100 to 33 m grid spacing. It indicates that the improvement of the model performance with resolution is not monotonical

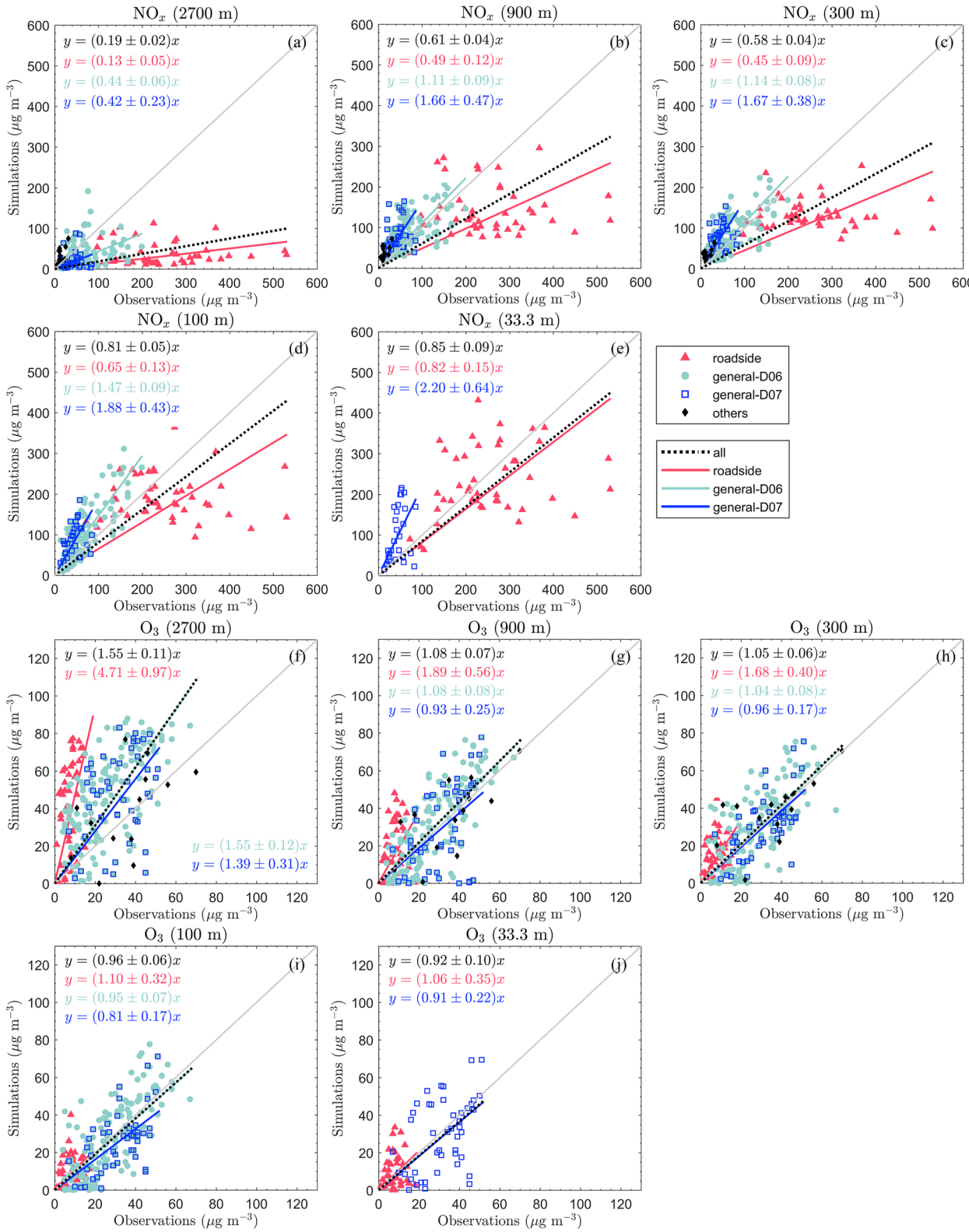

Figure 2. Correlation between simulated (a–e) NO_X and (f–j) ozone at different spatial resolutions (D03, 2,700 m; D04, 900 m; D05, 300 m; D06, 100 m; and D07, 33.3 m) against surface monitoring data. Cyan dots are for the general sites covered by D06; black diamonds are for the other general sites out of D06; blue squares are for the three general sites covered by D07; red triangles are for roadside sites. Cyan, blue, and red solid lines are the linear regressions of the D06 covered general sites, D07 covered general sites, and roadside sites, respectively, and black dash lines are the fits of all the sites. Note that, different domains cover different numbers of sites.

Table 1
Statistical Parameters Adopted to Evaluate the Simulated NO_X and Ozone Concentration Values Versus Surface Measurements at Air Quality Monitoring Stations in Hong Kong

		Nitrogen dioxide (NO_X)			Ozone (O_3)		
Stations	Model resolution (m)	MB (μg m^{-3})	RMSE (μg m^{-3})	*r*	MB (μg m^{-3})	RMSE (μg m^{-3})	*r*
All	2,700	−64.7	117.4	0.152	21.9	30.4	0.445
	900	−7.4	81.9	0.556	3.5	15.9	0.677
	300	−10.3	81.5	0.574	2.8	13.6	0.712
	100	12.2	76.5	0.651	−0.8	12.7	0.739
	33	10.9	**104.0**	**0.622**	−0.1	**14.1**	**0.639**
General-D06	2,700	−29.2	49.4	0.310	19.9	27.5	0.545
	900	18.5	41.4	0.553	2.4	15.7	0.694
	300	18.6	40.5	0.605	1.6	13.9	0.700
	100	**33.0**	**52.2**	0.769	−1.5	13.5	0.717
	33	–	–	–	–	–	–
General-D07	2,700	−22.2	35.9	0.008	15.8	27.3	0.308
	900	40.7	56.1	0.040	−1.8	19.7	0.462
	300	38.4	49.1	0.289	−1.0	13.1	0.637
	100	**47.1**	**59.6**	0.335	**−5.9**	**14.6**	**0.583**
	33	**57.9**	**85.1**	0.402	−2.1	**17.5**	**0.442**
Roadside	2,700	−213.7	239.6	−0.106	35.2	41.6	0.296
	900	−107.6	161.3	−0.044	9.2	16.9	0.220
	300	−120.5	161.2	0.056	7.3	12.2	0.281
	100	−61.0	129.8	0.031	2.2	8.6	**0.185**
	33	−20.5	114.9	0.277	2.1	**9.4**	**0.124**

Note. The Mean Bias (MB) and the Root Mean Square Error (RMSE) are in μg m^{-3}. The correlation coefficient (*r*) is unitless. The bolded values represent cases in which the increased resolution leads to a worse score. The stations are cataloged to all the stations covered by each domain (All), general stations covered by D06 (General-D06), general stations covered by D07 (General-D07), and roadside stations (Roadside).

in the case of O_3. This is possibly due to the accumulated errors in the long-distance transport when passing through the nested domains, which has a larger influence on the longer-lived species such as ozone than on the species with shorter lifetime (e.g., NO_X). This is consistent with the changes in the slope of the linear regression line. The situation is different for NO_X when considering the roadside stations: the MB and RMSE are lower, and the correlation coefficient is higher at 33 m than at 100 m resolution. This indicates that the local variation represents the dominant factor controlling the NO_X concentration distribution in the polluted areas, and therefore the high-resolution model provides a better representation of the measured values.

When considering all stations as well as the general stations, the RMSE for NO_X and for ozone increases and the correlation coefficient decreases when the model resolution is enhanced from 100 to 33 m. In other words, the model performance is best at the resolution of 100 m. If only considering the general stations that are distant from the pollution sources, the best model results are found at 100–300 m resolution, revealing a larger influence from transport when the local emissions are weaker. Additionally, the correlation coefficient for NO_X continues to increase with the model resolution, although the MB and RMSE become larger beyond 300 m resolution. This implies that the high model resolution may produce a larger bias due to some limitations (e.g., errors in the emission inventory); however, the variations in the measurements are more realistically reproduced.

In addition to the direct comparison obtained by extracting the nearest grid points of the model results to the measurement stations, we also provide downsampling evaluation (coarse evaluation; see details in Text S2 and Tables S3–S5 in Supporting Information S1). It shows that the calculated MBs and RSMEs for the roadside

stations from the averaged high-resolution LES become larger when averaging the results to the coarser resolutions. It indicates that the roadside measurements represent a local situation in a relatively small area. In the case of the general stations, the calculated statistics do not change significantly due to the averaging, which means that those stations are representing of a larger area than the roadside stations. However, the conclusion remains the same: the models obtain more information through resolving more detailed physical and chemical processes when the grid spacing is decreased.

The calculated statistical parameters for the meteorological variables (temperature, wind speed, and wind direction) are provided in Table S6 in Supporting Information S1. The correlation plots are shown in Figures S4–S6 in Supporting Information S1. The comparison of the station-averaged diurnal variations is in Figure S7 in Supporting Information S1. If only considering the stations covered by all the domains (referred to as D07 in Table S6 in Supporting Information S1), the smallest MB and RMSE for temperature are found at the model resolution of 900 m, indicating that increasing the model resolution does not provide better temperature predictions. However, the MB associated with the wind field becomes smaller when the grid spacing goes down to 33 m, and the RMSE is smallest at 100 m resolution. This implies that the LES provides some improvements in the wind prediction, which is important for the pollution transport and dispersion, although the correlation is weak (see more interpretations in Text S3 in Supporting Information S1). This is, on the one hand, because of the complex turbulent flows in the high-density built area, where the building morphology has a significant impact on the local wind fields. On the other hand, the number of the stations in the city center is limited. Therefore, the parameters are also calculated with more stations that covered by D06. The obtained statistics for D06 provide the same conclusion with that for D07, and the correlation coefficients become larger and increase with the model resolution. Combining the evaluations of the modeled chemical species and meteorological variables indicates that the improvements in the wind fields in the high-resolution models have some contribution to the quality of the chemical predictions, while a better representation of the emissions plays a more important role in predicting the pollutant distributions near the roads.

4. Conclusions

In this study we analyze the role of increasing model spatial resolution in the air quality simulations in a polluted urban region. The model experiments are performed in the megacity Hong Kong, where the terrain and land use are complex, and the air pollution is severe with multi-type sources. Various model resolutions are adopted in the simulations with several nested domains, among which the innermost three domains are calculated by the LES method. In addition to the direct comparison between the modeled and measured values of the chemical species at the surface stations, a statistical analysis is conducted for an objective evaluation. To examine the best model results for different conditions, the station types are divided between roadside stations near the traffic emissions and general stations that are located at a distance from the pollution sources.

The comparison between measured and simulated NO_X and O_3 concentrations at Central Station on a busy road shows that the results from the high-resolution model are characterized by stronger variations in the time series caused by the turbulent flows and reproduce better the extreme values in the observations. The agreement between simulations and measurements improves as the model resolution increases, and the 33-m LES provides the best results.

The statistical analysis indicates that the best model performance for the general stations is with the model resolution of 100–300 m, at which the influence from the transport and local emissions are equivalent. A further increase of the resolution to 33 m does not lead to better results at the general stations. However, the model with the highest resolution obtains the best representation of the NO_X concentrations at the roadside stations, implying that the strength of the emissions is the control factor of the distribution of the primary pollutants. As for O_3 with a longer lifetime, the improvement with the 33-m simulation is limited even for the roadside stations.

This study confirms the advantages of increasing model resolution to LES scales for urban areas with complex terrain, diverse land-use types, and intense pollution sources, especially when the emissions are heterogeneously distributed. The improvements with resolution reach the limit when the accumulated errors from transport start to overtake the local emissions. Therefore, the best resolution differs with species and locations, and the model resolution should be chosen specifically for the focused species and study area.

Data Availability Statement

The WRF model is publicly available at WRF (2023). The air quality data at surface stations are publicly available on the Hong Kong EPD website (EPD, 2023). The model results shown in this work are available at Ma (2023).

Acknowledgments
This research is supported by the Hong Kong Research Grants Council (Grant T24-504/17-N). Yong-Feng Ma's contribution to this work has been supported by the National Natural Science Foundation of China (NSFC Award 42075078). The National Center for Atmospheric Research is sponsored by the US National Science Foundation. We would like to acknowledge high-performance computing support from NCAR Cheyenne. Open Access funding enabled and organized by Projekt DEAL.

References

Deardorff, J. W. (1970). A numerical study of three-dimensional turbulent channel flow at large Reynolds numbers. *Journal of Fluid Mechanics*, *41*(2), 453–480. https://doi.org/10.1017/S0022112070000691

EPD. (2023). Environmental Protection Department Air Quality Data – Download/display [Dataset]. Stl. Retrieved from https://cd.epic.epd.gov.hk/EPICDI/air/station/?lang=_en

Falasca, S., & Curci, G. (2018). High-resolution air quality modeling: Sensitivity tests to horizontal resolution and urban canopy with WRF-CHIMERE. *Atmospheric Environment*, *187*, 241–254. https://doi.org/10.1016/j.atmosenv.2018.05.048

Flemming, J., Huijnen, V., Arteta, J., Bechtold, P., Beljaars, A., Blechschmidt, A. M., et al. (2015). Tropospheric chemistry in the integrated forecasting system of ECMWF. *Geoscientific Model Development*, *8*(4), 975–1003. https://doi.org/10.5194/gmd-8-975-2015

Grell, G. A., Peckham, S. E., Schmitz, R., McKeen, S. A., Frost, G., Skamarock, W. C., & Eder, B. (2005). Fully coupled "online" chemistry within the WRF model. *Atmospheric Environment*, *39*(37), 6957–6975. https://doi.org/10.1016/j.atmosenv.2005.04.027

Guillas, S., Bao, J., Choi, Y., & Wang, Y. (2008). Statistical correction and downscaling of chemical transport model ozone forecasts over Atlanta. *Atmospheric Environment*, *42*(6), 1338–1348. https://doi.org/10.1016/j.atmosenv.2007.10.027

Hong, S.-Y., Noh, Y., & Dudhia, J. (2006). A new vertical diffusion package with an explicit treatment of entrainment processes. *Monthly Weather Review*, *134*(9), 2318–2341. https://doi.org/10.1175/mwr3199.1

Joe, D. K., Zhang, H., DeNero, S. P., Lee, H.-H., Chen, S.-H., McDonald, B. C., et al. (2014). Implementation of a high-resolution source-oriented WRF/chem model at the Port of Oakland. *Atmospheric Environment*, *82*, 351–363. https://doi.org/10.1016/j.atmosenv.2013.09.055

Khan, B., Banzhaf, S., Chan, E. C., Forkel, R., Kanani-Sühring, F., Ketelsen, K., et al. (2021). Development of an atmospheric chemistry model coupled to the PALM model system 6.0: Implementation and first applications. *Geoscientific Model Development*, *14*(2), 1171–1193. https://doi.org/10.5194/gmd-14-1171-2021

Kim, Y., Wu, Y., Seigneur, C., & Roustan, Y. (2018). Multi-scale modeling of urban air pollution: Development and application of a street-in-grid model (v1.0) by coupling MUNICH (v1.0) and Polair3D (v1.8.1). *Geoscientific Model Development*, *11*(2), 611–629. https://doi.org/10.5194/gmd-11-611-2018

Kwak, K.-H., Baik, J.-J., Ryu, Y.-H., & Lee, S.-H. (2015). Urban air quality simulation in a high-rise building area using a CFD model coupled with mesoscale meteorological and chemistry-transport models. *Atmospheric Environment*, *100*, 167–177. https://doi.org/10.1016/j.atmosenv.2014.10.059

Lugon, L., Sartelet, K., Kim, Y., Vigneron, J., & Chrétien, O. (2020). Nonstationary modeling of NO_2, NO and NOx in Paris using the street-in-grid model: Coupling local and regional scales with a two-way dynamic approach. *Atmospheric Chemistry and Physics*, *20*(13), 7717–7740. https://doi.org/10.5194/acp-20-7717-2020

Ma, Y.-F. (2023). Comparison between WRF simulations and air quality data in Hong Kong [Dataset]. GitHub. Retrieved from https://github.com/Youssef-yfma/WRF-LES-Chem_output_HK.git

Mass, C. F., Ovens, D., Westrick, K., & Colle, B. A. (2002). Does increasing horizontal resolution produce more skillful forecasts? *Bulletin of the American Meteorological Society*, *83*(3), 407–430. https://doi.org/10.1175/1520-0477(2002)083<0407:DIHRPM>2.3.Co;2

Muñoz-Esparza, D., Lundquist, J. K., Sauer, J. A., Kosović, B., & Linn, R. R. (2017). Coupled mesoscale-LES modeling of a diurnal cycle during the CWEX-13 field campaign: From weather to boundary-layer eddies. *Journal of Advances in Modeling Earth Systems*, *9*(3), 1572–1594. https://doi.org/10.1002/2017MS000960

Pfister, G. G., Eastham, S. D., Arellano, A. F., Aumont, B., Barsanti, K. C., Barth, M. C., et al. (2020). The multi-scale infrastructure for chemistry and aerosols (MUSICA). *Bulletin of the American Meteorological Society*, *101*(10), E1743–E1760. https://doi.org/10.1175/BAMS-D-19-0331.1

Skamarock, W. C., Klemp, J. B., Dudhia, J., Gill, D. O., Liu, Z., Berner, J., et al. (2019). *A description of the advanced research WRF Model version 4.1*. National Center for Atmospheric Research, Technical Notes, NCAR/TN-556+STR (p. 145). https://doi.org/10.5065/1dfh-6p97

Stockwell, W. R., Middleton, P., Chang, J. S., & Tang, X. (1990). The second generation regional acid deposition model chemical mechanism for regional air quality modeling. *Journal of Geophysical Research*, *95*(D10), 16343–16367. https://doi.org/10.1029/JD095iD10p16343

Thomas, A. M., & Kurzeja, R. J. (2023). Realistic large eddy and dispersion simulation experiments during project sagebrush phase 1. *Atmospheric Environment*, *312*, 120030. https://doi.org/10.1016/j.atmosenv.2023.120030

Valari, M., & Menut, L. (2008). Does an increase in air quality models' resolution bring surface ozone concentrations closer to reality? *Journal of Atmospheric and Oceanic Technology*, *25*(11), 1955–1968. https://doi.org/10.1175/2008jtecha1123.1

Wang, T., Li, J., Pan, J., Ji, D., Kim, Y., Wu, L., et al. (2022). An integrated air quality modeling system coupling regional-urban and street models in Beijing. *Urban Climate*, *43*, 101143. https://doi.org/10.1016/j.uclim.2022.101143

Wang, Y., Brasseur, G. P., & Wang, T. (2022). Segregation of atmospheric oxidants in turbulent urban environments. *Atmosphere*, *13*(2), 315. https://doi.org/10.3390/atmos13020315

Wang, Y., Ma, Y.-F., Muñoz-Esparza, D., Dai, J., Li, C. W. Y., Lichtig, P., et al. (2023). Coupled mesoscale-microscale modeling of air quality in a polluted city using WRF-LES-Chem. *Atmospheric Chemistry and Physics*, *23*(10), 5905–5927. https://doi.org/10.5194/acp-23-5905-2023

Wang, Y., Ma, Y.-F., Muñoz-Esparza, D., Li, C. W. Y., Barth, M., Wang, T., & Brasseur, G. P. (2021). The impact of inhomogeneous emissions and topography on ozone photochemistry in the vicinity of Hong Kong Island. *Atmospheric Chemistry and Physics*, *21*(5), 3531–3553. https://doi.org/10.5194/acp-21-3531-2021

WRF. (2023). Weather Research and Forecasting (WRF) model [Software]. GitHub. Retrieved from https://github.com/wrf-model/WRF/

Zheng, Y., Miao, Y., Liu, S., Chen, B., Zheng, H., & Wang, S. (2015). Simulating flow and dispersion by using WRF-CFD coupled model in a built-up area of Shenyang, China. *Advances in Meteorology*, *2015*, 528618. https://doi.org/10.1155/2015/528618

References From the Supporting Information

Bian, Y., Huang, Z., Ou, J., Zhong, Z., Xu, Y., Zhang, Z., et al. (2019). Evolution of anthropogenic air pollutant emissions in Guangdong Province, China, from 2006 to 2015. *Atmospheric Chemistry and Physics*, *19*(18), 11701–11719. https://doi.org/10.5194/acp-19-11701-2019

Hu, X. M., Nielsen-Gammon, J. W., & Zhang, F. (2010). Evaluation of three planetary boundary layer schemes in the WRF model. *Journal of Applied Meteorology and Climatology*, *49*(9), 1831–1844. https://doi.org/10.1175/2010JAMC2432.1

Johansson, L., Jalkanen, J.-P., & Kukkonen, J. (2017). Global assessment of shipping emissions in 2015 on a high spatial and temporal resolution. *Atmospheric Environment*, *167*, 403–415. https://doi.org/10.1016/j.atmosenv.2017.08.042

Li, M., Zhang, Q., Kurokawa, J. I., Woo, J. H., He, K., Lu, Z., et al. (2017). MIX: A mosaic Asian anthropogenic emission inventory under the international collaboration framework of the MICS-Asia and HTAP. *Atmospheric Chemistry and Physics*, *17*(2), 935–963. https://doi.org/10.5194/acp-17-935-2017

Sathyanadh, A., Prabha, T. V., Balaji, B., Resmi, E., & Karipot, A. (2017). Evaluation of WRF PBL parameterization schemes against direct observations during a dry event over the Ganges valley. *Atmospheric Research*, *193*, 125–141. https://doi.org/10.1016/j.atmosres.2017.02.016

Zhang, B. H., Liu, S. H., Liu, H. P., & Ma, Y. J. (2012). The effect of MYJ and YSU schemes on the simulation of boundary layer meteorological factors of WRF. *Chinese Journal of Geophysics*, *55*, 2239–2248. https://doi.org/10.6038/j.issn.0001-5733.2012.07.010

Zheng, B., Tong, D., Li, M., Liu, F., Hong, C., Geng, G., et al. (2018). Trends in China's anthropogenic emissions since 2010 as the consequence of clean air actions. *Atmospheric Chemistry and Physics*, *18*(19), 14095–14111. https://doi.org/10.5194/acp-18-14095-2018

Zheng, J., Zhang, L., Che, W., Zheng, Z., & Yin, S. (2009). A highly resolved temporal and spatial air pollutant emission inventory for the Pearl River Delta region, China and its uncertainty assessment. *Atmospheric Environment*, *43*(32), 5112–5122. https://doi.org/10.1016/j.atmosenv.2009.04.060